Eur. Phys. J. D **16**, 115–118 (2001)

THE EUROPEAN PHYSICAL JOURNAL D
EDP Sciences
© Società Italiana di Fisica
Springer-Verlag 2001

Measuring the implantation depth of silver clusters in graphite

D.J. Kenny[1,a], S.C. Weller[1], M. Couillard[1], R.E. Palmer[1], C.F. Sanz-Navarro[2], and R. Smith[2]

[1] Nanoscale Physics Research Laboratory, School of Physics and Astronomy, The University of Birmingham, Birmingham, B15 2TT, UK
[2] School of Mathematics and Physics, Loughborough University, Loughborough, Leicestershire, LE11 3TU, UK

Received 30 November 2000

Abstract. Scanning tunnelling microscopy (STM) and molecular dynamics (MD) simulations have been used to investigate the implantation of Ag_7^- clusters into the graphite surface. An experimental measure of the implantation depth of individual clusters is gained *via* thermal oxidation of the bombarded graphite surfaces. This process results in etching of the cluster-induced defects to form etch pits which grow laterally whilst retaining the depth of the implanted cluster. STM imaging of the etch pits reveals the distribution of implantation depths for deposition energies of 2 keV and 5 keV. Molecular dynamics simulations for clusters of 5 keV energy show that the implantation depth for Ag_7^- is largely independent of the impact site on the graphite surface and the cluster orientation. The implantation depth found by MD lies at the upper edge of the experimental depth distribution.

PACS. 36.40.-c Atomic and molecular clusters – 68.37.Ef Scanning tunnelling microscopy (including chemistry induced with STM) – 02.70.Ns Molecular dynamics and particle methods

1 Introduction

One of the opportunities which arises from the use of mass-selected cluster beams in the fabrication of nanomaterials, when compared with the self-assembly of passivated nanoparticles [1], is the exploitation of the controllable kinetic energy of the ionised cluster beam to create well-defined "vertical" nanostructures *via* implantation of clusters into a substrate. Such structures may be of interest, for example, in the field of catalysis, since pinned, monodispersed arrays of clusters show catalytic properties dependent upon the cluster size [2,3]. Low energy cluster deposition on the graphite surface (*i.e.* soft landing) leads to diffusion and aggregation of the clusters to form larger particles on the surface [4,5]. At intermediate energies it is possible to pin an incoming cluster at its impact site *via* the removal of one or more carbon atoms, *i.e.* through the formation of a surface defect [6], thus preventing the cluster from diffusing on the surface. Recent molecular dynamics (MD) simulations of high energy deposition [7,8] have predicted the formation of "cluster down a well" structures, *via* the impact of energetic Ag and Si clusters ($N = 20 - 200$) on the graphite surface. In these simulations the implantation depth, D, scaled as $D = E/N^{2/3}$ (where E is the impact energy and N is the number of atoms) and the clusters were ultimately located at the bottom of an open hole "drilled" in the graphite surface (with diameter determined by the diameter of the cluster itself). This suggests the possibility of producing a more thermally stable variant of a monodispersed cluster array by locating each cluster at the bottom of its own well. However, since the well diameters produced by small clusters, of the order 1-2 nm, are typically much smaller than the diameter of an STM tip, experimental measurements of the depth of the implantation structure require that the feature is "opened up" (by etching) prior to STM measurement.

In this paper we present a combined experimental and MD study of the implantation depth of Ag_7^- clusters in graphite. Oxidation of the graphite substrate in a furnace after cluster implantation leads to the creation of etch pits, located at each impact site, with the same depth as the implanted cluster. Oxidation of graphite surfaces has been investigated over a long period [9], but this technique has only recently been utilised as a mechanism for determining the implantation depths of charged particles such as atomic ions [10] and ionised clusters [11]. Specific experiments include measurements of the implantation depths of charged proteins [12], fullerene molecules [13] and positively charged Ta clusters [14] in the graphite surface.

2 Experimental

Silver clusters were formed using a negative-ion beam cluster source based on the sputtering of a metal target by Cs^+ ions. Details of this (low-mass) cluster source have been published in full elsewhere [15]. Silver clusters were size-selected to give Ag_7^- and deposited onto highly oriented

[a] e-mail: D.J.Kenny@bham.ac.uk

pyrolitic graphite (HOPG) substrates at normal incidence. The base pressure in the high vacuum deposition chamber of the cluster source was 5×10^{-8} mbar. HOPG samples were prepared by cleaving with sticky tape immediately prior to insertion into vacuum. After cluster deposition, oxidative etching was accomplished by inserting the samples into a furnace at an operating temperature of 650 °C under ambient atmospheric conditions for periods ranging from 3-5 minutes. Following oxidation, the HOPG samples were transferred from the furnace and allowed to cool before imaging under ambient conditions by benchtop STM (Rasterscope^{TM} 4000) operating in constant current mode with mechanically cut Pt/Ir tips.

3 Results

Fig. 1 shows two examples of the oxidised graphite surface obtained after implantation of Ag_7^- clusters at deposition energies of 2 keV, fig. 1(a), and 5 keV, fig. 1(b). Both images show the etch pits created by the etching process, and in both cases a distribution of etch pit depths is evident. Perhaps the most striking observation in fig. 1(a) is the large variation in the etch pit diameters. The reason for this is that the lateral etch rate is a function of the depth of the initial defect, with deeper pits etching faster than shallower pits up to a depth of approximately 4 monolayers (ML); beyond this depth the etch rate is nearly independent of depth [16]. What is also apparent is that the smaller, shallower pits are typically almost spherical in shape whereas the deeper pits appear hexagonal (reflecting the hexagonal atomic structure of the graphite (0001) surface). It is clear from fig. 1(b), obtained after Ag_7^- deposited at the higher kinetic energy of 5 keV, that the majority of pits in this case are hexagonal in shape and that the size distribution of pit diameters is much smaller. This reflects the fact that the etch rate is independent of depth for these deeper pits. An interesting observation that can be seen in both STM images is that certain pits contain a second inner pit near the centre, which is generally 1 to 2 ML deeper. We believe that this secondary structure may arise from clusters which slightly damage the atomic layer below their final resting position, to create a defect smaller than the cluster diameter. Such a defect would give rise to a slow lateral etching rate and create the type of inner etch pit observed in fig. 1. From a quantitative point of view, the depths of the etch pits are readily measured by taking a line profile across them. An example of such a profile, taken along the line indicated in fig. 1(b), is displayed in fig. 1(c) which shows four pits of depth 5, 10, 8 and 7 ML, respectively, moving from left to right.

After imaging of the samples with STM, etch pit depths were measured and collated to produce histograms showing the frequency of occurrence of each depth. The depths of those features with a secondary pit near the centre were measured to the bottom of this inner pit. Figs. 2(a) and 3(a) show the raw depth distributions for deposition energies of 2 keV and 5 keV, respectively. Because the graphite surface has naturally occurring defects

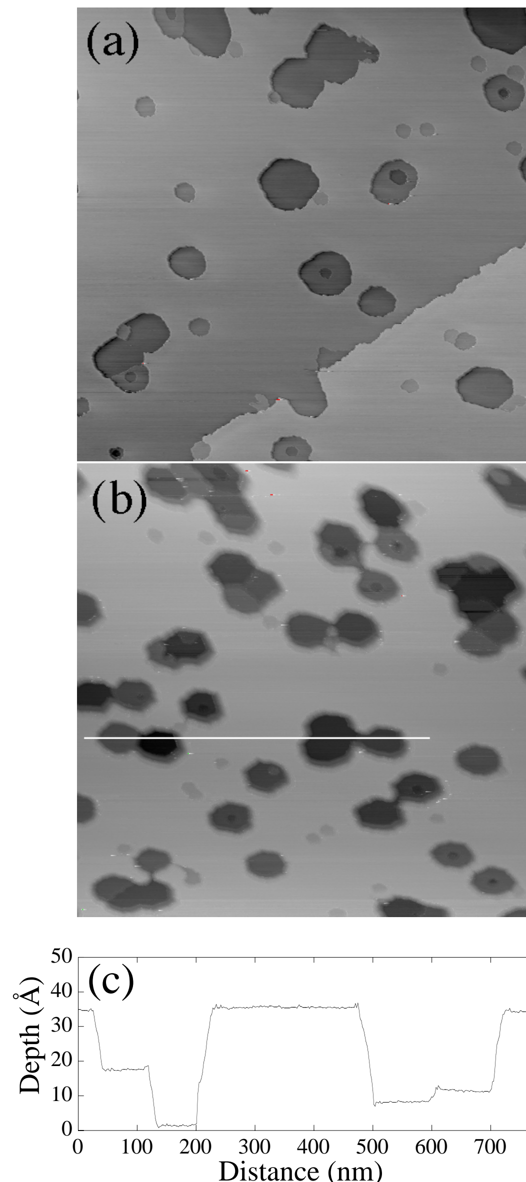

Fig. 1. STM images of oxidatively etched graphite after implantation into graphite of Ag_7^- cluster ions at energies of (a) 2 keV (image size 1.5 μm × 1.5 μm), and (b) 5 keV (1.0 μm × 1.0 μm). Tunnelling conditions employed in both cases were +0.4 V on the sample and 0.4 nA. (c) A height profile along the line indicated in (b) showing pits of depth 5, 10, 8 and 7 ML (1 ML = 3.35 Å).

(*i.e.* in addition to the defects formed by cluster bombardment), there is a resultant "background" of monolayer pits on each sample. This phenomenon is clearly seen in both fig. 2(a) and fig. 3(a) as a peak at 1 ML in addition to the "main" peak relating to the "average" implantation depth of the clusters. These background 1 ML pits are more difficult to distinguish from cluster pits at the deposition energy of 2 keV, because in this case a substantial number of the 1 ML pits in the histogram result from cluster impact events. It is therefore necessary to be able to distinguish between the two. This problem is

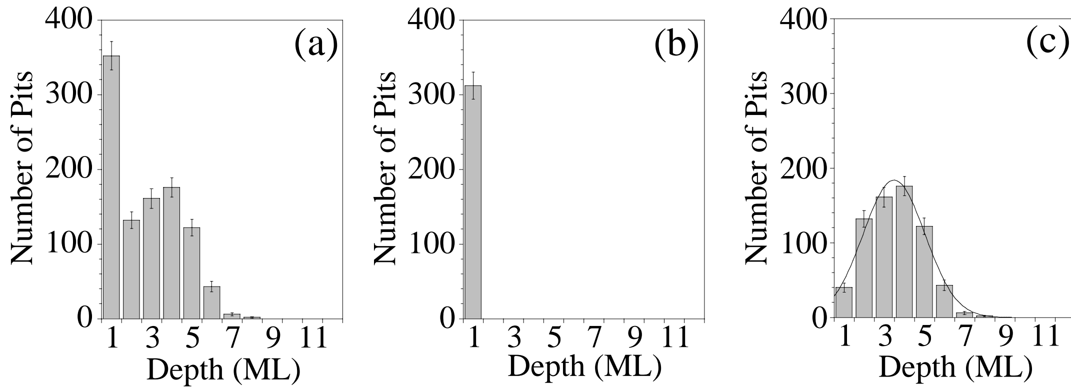

Fig. 2. Histogram of etch pit depths after implantation of Ag_7^- at 2 keV as measured by STM; (a) "raw data"; (b) the natural defects measured outside the cluster impact area leading to a background count of 1 ML pits; (c) Gaussian fit to background subtracted data.

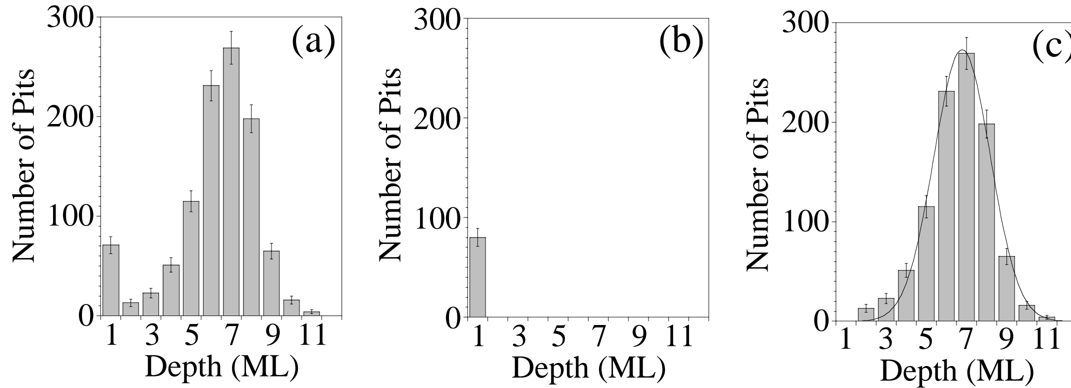

Fig. 3. Histogram of etch pit depths after implantation of Ag_7^- at 5 keV as measured by STM; (a) "raw data"; (b) the natural defects measured outside the cluster impact area leading to a background count of 1 ML pits; (c) Gaussian fit to background subtracted data.

overcome by taking STM images, for each graphite sample, in regions not exposed to the cluster beam, to obtain a background reading of the number of natural defects on each sample. Figs. 2(b) and 3(b) show histograms of the "background" pits taken for 2 keV and 5 keV samples, respectively. In the case of deposition at 5 keV, fig. 3(b), it is clear that all of the pits of 1 ML depth are due to natural defects as the background count agrees well with the monolayer peak seen in fig. 3(a) (all error bars come from Poisson counting, *i.e.*, $\sqrt{N}$ statistics). The resulting background-subtracted histograms, figs. 2(c) and 3(c), appear approximately Gaussian in form, although a slight skew towards the lower energy range is evident at 5 keV. A Gaussian curve was fitted to both histograms to determine a value for the "average" implantation depth at these energies. These Gaussian fits give a most common implantation depth of 3.9 ML (with a full width at half maximum (FWHM) of 3.3 ML) at 2 keV and 6.8 ML at 5 keV (with a FWHM of 3.6 ML). Further experimental measurements of this kind would allow a systematic investigation of the cluster implantation depth as a function of both cluster size and kinetic energy.

To complement the experimental measurements of the implantation depth of Ag_7^- clusters in graphite we have also modelled the cluster implantation process *via* MD simulation. Recent MD simulations of Ag_n implantation into graphite were concerned with larger clusters. Topics of particular interest, in the case of small cluster impact, are the roles of the cluster impact site and cluster orientation, as previously identified in the case of Ag_3^- impact on graphite [17,18].

Details of our MD code and the potentials used can be found elsewhere [7,8]. The size of the modelled graphite substrate is 50 Å × 50 Å with sixteen graphite layers. The simulations run for 1.5 ps, with a time step of 0.75 fs. The initial configuration of the (neutral) Ag_7 clusters in the simulation is found by minimising the potential energy function *via* a genetic algorithm [19]. The temperature of the simulation, which employs a thermostat [20], is 300 K. In total, twelve different simulations for the impact energy of 5 keV have been run which consider four different impact sites on the graphite surface and three different orientations of the Ag_7 cluster for each impact site. The simulations show that Ag_7 clusters always create a deep well inside the graphite substrate, as illustrated in fig. 4. The distribution of the total number of damaged layers, *i.e.* the implantation depth, obtained from the MD simulations is very narrow: a depth of 11 ML is obtained in

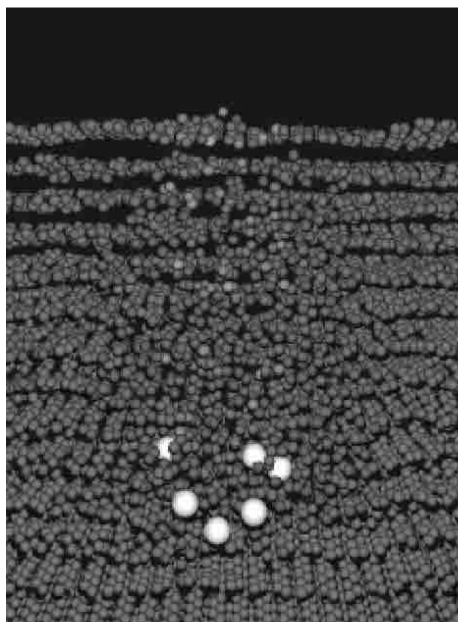

Fig. 4. A molecular dynamics simulation image showing the well created by an implanting Ag_7 cluster incident at 5 keV on the graphite substrate and its final resting position (light grey balls represent Ag atoms, dark grey balls represent C atoms).

seven of the simulations and 10 ML in the other five. The holes created in the 11th layer down are much smaller than those in the higher layers above, just sufficient to allow one or two Ag atoms to pass through and lie underneath. This is consistent with our proposed explanation regarding the production of secondary, inner etch pits.

The narrow depth distribution arising from the MD simulations suggests that, at least for the case of Ag_7^-, the different impact sites and orientation of the clusters have little effect on the ultimate implantation depth. Intriguingly, the implantation depth of 10-11 ML found in the simulations lies almost exactly at the upper edge of the experimental distribution for Ag_7^- implantation at 5 keV, fig. 3(c), whereas the peak of the experimental distribution lies at lower depths. This suggests that there are cluster energy loss channels operating in the experiment which are not included in the simulations, possibly associated with the cluster charge. This may open up an important area for future study.

4 Summary

We have investigated the implantation depths of Ag_7^- clusters using scanning tunnelling microscopy and molecular dynamics simulations. Oxidative etching of cluster bombarded surfaces results in the formation of etch pits which "open up" the cluster implantation track laterally for STM analysis. Thus STM imaging of the etched surfaces allows frequency distributions of etch pit depth to be plotted for implantation energies of 2 keV and 5 keV and reveals the most common implantation depths of 3.9 ML and 6.8 ML, respectively. Complementary molecular dynamics simulations show that the implantation depth for Ag_7^- is independent of the impact site and the cluster orientation. The implantation depth predicted by these simulations for a deposition energy of 5 keV is between 10-11 ML, close to the upper edge of the experimental depth distribution but significantly above the peak value.

We would like to thank the Engineering and Physical Sciences Research Council (EPSRC) for financial support of this work and the award of studentships to DJK and SCW. SCW would also like to thank Johnson Matthey for a CASE award. MC acknowledges the ORS Awards Scheme (UK), FCAR (Québec, Canada) and the School of Physics and Astronomy, University of Birmingham, for financial support.

References

1. P.J. Durston, J. Schmidt, R.E. Palmer, J.P. Wilcoxon, App. Phys. Lett. **71**, 2940 (1997).
2. A. Sanchez, S. Abbet, U. Heiz, W.-D. Schneider, H. Hakkinen, R.N. Barnett, U. Landman, J. Phys. Chem. A **103**, 9573 (1999).
3. M. Valden, X. Lai, D.W. Goodman, Science **281**, 1647 (1998).
4. I.M. Goldby, L. Kuipers, B. von Issendorff, R.E. Palmer, Appl. Phys. Lett. **69**, 2819 (1996).
5. S.J. Carroll, K. Seeger, R.E. Palmer, Appl. Phys. Lett. **72**, 305 (1998).
6. S.J. Carroll, S. Pratontep, M. Streun, R.E. Palmer, S. Hobday, R. Smith, J. Chem. Phys. **113**, 7723 (2000).
7. S.J. Carroll, P.D. Nellist, R.E. Palmer, S. Hobday, R. Smith, Phys. Rev. Lett. **84**, 2654 (2000).
8. R. Neuendorf, R.E. Palmer, R. Smith, Appl. Phys. Lett. **77**, 3003 (2000).
9. G.R. Henning, J. Chem. Phys. **40**, 169 (1964).
10. S.M. Lee, Y.H. Lee, Y.G. Hwang, J.R. Hahn, H. Kang, Phys. Rev. Lett. **82**, 217 (1999).
11. G. Bräuchle, S. Richard-Schneider, D. Illig, J. Rockenberger, R.D. Beck, M.M. Kappes, Appl. Phys. Lett. **67**, 52 (1995).
12. C.T. Reimann, P.A. Sullivan, A. Türpitz, S. Altmann, A.P. Quist, A. Bergman, S.O. Oscarsson, B.U.R. Sundqvist, P. Håkansson, Surf. Sci. **341**, L1019 (1995).
13. G. Bräuchle, S. Richard-Schneider, R.D. Beck, H. Schreiber, M.M. Kappes, Nuc. Instr. Meth. Phys. Res. B **112**, 105 (1996).
14. C.T. Reimann, S. Andersson, P. Brühwiler, N. Mårtensson, L. Olsson, R. Erlandsson, M. Henkel, H.M. Urbassek, Nuc. Instr. Meth. Phys. Res. B **140**, 159 (1998).
15. S.G. Hall, M.B. Nielsen, A.W. Robinson, R.E. Palmer, Rev. Sci. Instrum. **68**, 3335 (1997).
16. F. Stevens, L.A. Kolodny, T.P. Beebe Jr, J. Phys. Chem. B **102**, 10799 (1998).
17. S.J. Carroll, S.G. Hall, R.E. Palmer, R. Smith, Phys. Rev. Lett. **81**, 3715 (1998).
18. S.G. Hall, M.B. Nielsen, R.E. Palmer, J. Appl. Phys. **83**, 733 (1998).
19. S. Hobday, R. Smith, J. Chem. Soc. Faraday Trans. **93**, 3919 (1997).
20. H.J.C. Berendsen, J.P.M. Postma, W.F. van Gunsteren, A. DiNola, J.R. Haak, J. Chem. Phys. **81**, 3684 (1984).